Global NEST Journal, Vol 19, No 1, pp 49-56

Nature and adsorption capacity of banana leaf rim carbon

Chaithra P. and Bhat Ishwara J.*
Department of Chemistry, Mangalore University, Mangalagangothri-574199, India.
Received: 20/08/2016, Accepted: 19/10/2017, Available online: 23/11/2017
*to whom all correspondence should be addressed:
e-mail: bhatij@yahoo.com

Abstract

The activated charcoal (AC) was synthesized from banana leaf rim (BLR) through three activation methods; physical (BLRC), chemical (Z BLRC, zinc chloride) and microwave activation (MW BLRC). The AC was characterized using fourier transform infrared spectrometer (FT-IR), Thermogravimetric analysis (TGA) & Differential thermogravimetric analysis (DTA) instrument and Field emission scanning electron microscope (FE-SEM). The Z BLRC has better thermal stability and adsorbent character compared with BLRC or MW BLRC. The present work is confined to an investigation on the adsorption process of Malachite green dye onto BLRC,

Z BLRC & MW BLRC. Factors affecting adsorption process were studied and results that adsorption increases with concentration of dye, agitation time and temperature. This experimental data satisfied the Langmuir adsorption isotherm model. Second order kinetics holds good for the present adsorption process. Thermodynamic parameters were ($\Delta H^{\ddagger}$, $\Delta S^{\ddagger}$ & $\Delta G^{\ddagger}$) evaluated. Based on the characterization and adsorption experimental result it may be concluded that Z BLRC has better adsorption capacity than BLRC or MW BLRC.

Keywords: Adsorption, Activated charcoal, malachite green, adsorption kinetics

1. Introduction

Adsorption is a process of accumulation of gas, liquid or solid particles on the surface of a solid. The substance which is adsorbed on the surface is known as adsorbate, whereas surface on which molecules adsorbed are known as adsorbent (Adamson, 1990). Activated charcoal (AC) or carbon has an ideal adsorbent character due to the presence of surface active center (micro, meso and macro pores), surface functional groups and surface charges (Bharathi and Ramesh, 2013). Activated carbon prepared from agricultural waste materials has much importance due to low cost for its raw materials and it is environmental friendly. Researchers investigated the adsorption of environmentally harmful synthetic dye onto activated carbon from agricultural waste products such as straw, rice husk, date pit, banana peel etc. (Kannan N. and Sundaram, 2001; Malik and Saha (2003); Mahmoudi *et al.*, 2014; Annadurai *et al.*, 2002). The literature revealed that adsorption of malachite green onto activated carbon prepared from rubber seed coat, thespesia populnea bark, rice husk, durian seed have been studied by Idris *et al.*, 2011; Prabakaran and Arivoli, 2012; Rahman *et al.*, 2005 and Ahmad *et al.*, 2014.

The present work involves synthesis of activated carbon from banana leaf rim (BLR) using three different activation methods; physical (BLRC), chemical (zinc chloride (Z BLRC)) and microwave activation (MW BLRC). The synthesized AC's (BLRC, Z BLRC & MW BLRC) were characterized using Fourier transform infrared spectrophotometer (FT-IR),Thermogravimetric analysis (TA) & Differential thermal analysis (DTA) and Field emission scanning electron microscope instruments. The present study investigates the malachite green adsorption onto BLRC, ZBLRC & MW BLRC. The adsorption study mainly deals with the adsorption isotherms (Freundlich & Langmuir adsorption isotherm), kinetics of adsorption (First-order and second-order kinetics) and thermodynamics of adsorption (thermodynamic parameters $\Delta H^{\ddagger}$, $\Delta S^{\ddagger}$ and $\Delta G^{\ddagger}$).

2. Materials and methods

2.1. Activated charcoal as an adsorbent

The activated charcoal was synthesized from the dried banana leaf rim (BLR) collected from agricultural field. In order to achieve porosity on the surface of the BLR, first it is subjected to carbonization. It results porous char but for the adsorption process this porosity has to be enhanced or activated. Therefore it is activated by three methods that are physical, chemical (zinc chloride) and microwave activation method. The physical and chemical (zinc chloride) activation in muffle furnace (300 °C, 2h.). Microwave activation (80 W, 280 min) in domestic micro oven. The activated charcoal obtained so was crushed in mortar to become powder and it was sieved to 250 µm to get uniform sized activated carbon.

2.2. Synthetic dye as an Adsorbate

The adsorbate material used in the present work is malachite green oxalate powder purchased from Sisco Research Laboratories Pvt.Ltd. Mumbai, India. Malachite green oxalate is a basic dye with the molecular structure as shown in Fig. 1.

The Malachite green oxalate is lustrous green crystal, soluble in water and methanol. Molecular formula $C_{52}H_{54}N_4O_{12}$ and molecular weight is 927.02g/mol. The aqueous solutions of the dye were prepared in distilled water. λ_{max} was determined using UV-Visible spectrophotometer and is found to 618nm.

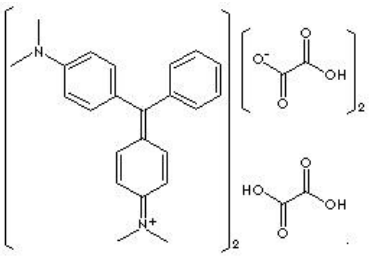

Figure 1. Molecular structure of Malachite green oxalate

2.3. FT-IR Analysis

Fourier transform infrared spectrophotometer (Shimadzu FT-IR Prestige-21, ATR method) was used to record the surface functional groups present in the raw and synthesized samples. The FT-IR spectra were recorded in wavenumber range of 4000-500 cm

2.4. TGA-DTA Analysis

Thermal stability of BLR, BLRC, ZBLRC, MWBLRC, samples was studied by thermogravimetric analysis (TA) and differential thermogravimetric analysis (DTA) using a TA-STD Q600 instrument under dry nitrogen atmosphere at the flow rate of 100 mL/min. The samples were heated from room temperature to 700 °C at predetermined rate of 20 °C/min.

2.5. FE-SEM Analysis

The surface image was scanned using Carl Zeiss Field emission scanning electron microscope. The SEM magnification was 2.50 KX and EHT=5.00 kV.

2.6. Adsorption Studies

The adsorption process was carried out by adding 0.1 g of activated carbon (BLRC, Z BLRC & MW BLRC) to a three beaker containing 50 ml of a malachite green solution of known concentration (C_0) and was stirred for 1h. The concentration of dye solution after the adsorption process was measured using UV-Spectrophotometer with λ_{max}=618 nm. The adsorption process was studied by varying the concentration of adsorbate C_0 (mg/L), contact time t (min) and temperature $T(K)$. The amount of dye adsorbed per unit mass of activated carbon and percentage obtained were calculated as follows (Zhang *et al.*, 2016).

$$q = \frac{(C_0 - C_e)V}{W} \quad (1)$$

Where C_0 is the initial concentration of dye (mg/L); C_e is the concentration of dye in the solution after adsorption (mg/L); V is the volume of the solution (ml); and W is the weight of activated carbon (g).

3. Results and discussion

3.1. FT-IR Analysis

The FT-IR spectra of banana leaf rim and activated charcoal samples were shown in Fig. 2a. & Fig. 2b. The FT-IR spectra of banana leaf rim shows characteristic peaks at 3531, 2922 and 2852 cm^{-1} this corresponds to intermolecular hydrogen bonded O-H stretching vibration and C-H stretching in alkane respectively. IR bands at 1822cm^{-1} to 1637 cm^{-1} this is due to C=O stretching [might be of anhydride, ester (γ-lactone), 1,4-Quinone and carboxylic acid groups]. The stretching frequency at 1455cm^{-1}, 1313cm^{-1}, 1180cm^{-1} and 1008cm^{-1} respectively due to C-H bending (-CH_3), C-N vibration (amines), S=O stretching (sulfonamides) and C-O-C stretching (ether). The IR peaks at 1000cm^{-1} to 750cm^{-1} is due to C-H out of plane bending (Pavia *et al.*, 2011; Dewan, 2010; Dyer, 1987).

The FT-IR spectra of BLRC, Z BLRC & MW BLRC was as shown in Fig. 2b. The FT-IR spectrum of banana leaf rim (Fig. 2a.) showed more IR peaks than its activated carbon samples (Fig. 4.). The O-H and C-H stretching recorded in FT-IR spectrum of raw sample at 2922cm^{-1} and 2852 cm^{-1} were not detected in the FT-IR spectra of BLRC, ZBLRC and MW BLRC. This indicates that structural changes observed between the banana leaf rim (BLR) and activated carbon due to the decomposition of some of the functional groups present in the raw material during activation process. Characteristic infrared absorptions of functional groups recorded in BLRC, Z BLRC and MW BLRC were shown in Table 1.

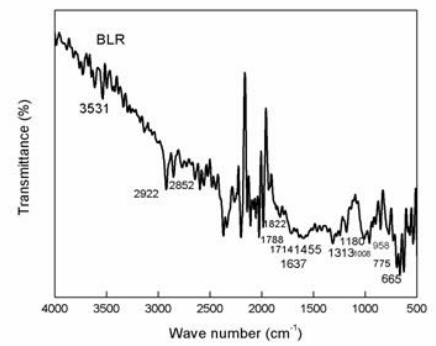

(2a)

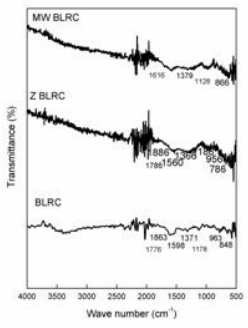

(2b)

Figure 2. 2a. FT-IR spectrum of banana leaf rim, **2b.** FT-IR spectra of BLRC, Z BLRC & MW BLRC

3.2. TGA-DTA Analysis

The thermal stability of BLR, BLRC, Z BLRC and MW BLRC was studied using Thermogravimetric analysis (TGA) and Differential thermogravimetric analysis (DTA). The TGA plot and its differential thermogravimetric plot of BLR, BLRC, Z BLRC & MW BLRC are shown in Fig. 3.

Table 1. Characteristic infrared absorptions of functional groups recorded in BLRC, Z BLRC and MW BLRC

Functional group	Intensity range (cm^{-1})
A. Hydrocarbon	
1. C-H out of plane bending	1000-750
2. C=C stretching, Aromatic alkene	1600-1500
B. Carbonyl groups(C=O)	
1. **Ester** stretching vibration, (γ- lactone)	1786,1776
2. Carboxylic acids (carboxylate anion stretching)	1610-1550
3. Anhydride stretching vibration	1886, 1863
C. Miscellaneous groups	
1. Amines, **C-N** vibration Primary, Secondary and tertiary	1360-1310
2. Sulfonamides, S=O stretching vibration	1188, 1178

The thermal decomposition of banana leaf rim was examined using thermogram curve i.e, (%) weight loss was recorded as a function of temperature (°C). TG curve of BLR (Fig. 3a.) reveals that till 200°C there was only 10.27% weight loss due to the moisture present on the surface. It has two knees before fully decomposed into ash indicating the two stability region and the decomposition of the system. The DTA curve of BLR (Fig. 3a.) also support the two degradation steps as it was seen in TG plot. The two decomposition temperature observed at 374.41 °C and 478.34 °C.

The TG curve of BLRC (Fig. 3b.) reveals that only 2.77 % of moisture evaporation occurs till 200 °C. The maximum decomposition region of the volatile matter was observed at 300-500 °C. The DTA curve showed single derivative peak at maximum decomposition temperature at 470.80 °C. This shows the presence of negligible amounts of hemicellulose in BLRC. The cellulose component degradation was found in TG curve between the temperature range 300 - 400 °C (Ouajai and Shanks, 2005). The final ash content was observed at 700 °C (13.05 %). It is clear from the TG curve of Z BLRC, that even at 200 °C the moisture content appeared to be high. This was mainly due to the reaction of zinc chloride with water. Thermal decomposition at 200-500 °C is mainly due to the decomposition of lignocellulose species. The DTA curve (Fig. 3c.) indicated the presence of two decomposition peaks at temperature 461.46 °C and 589.29 °C.

Thermal decomposition of MW BLRC (Fig. 3d.) showed the presence of three degradation steps. There three steps indicate the evaporation of moisture (step 1: 200 °C), decomposition of hemi cellulose and cellulose (step 2: 200 to 400 °C) and decomposition of carbonyl groups (step3: 400 to 500 °C). DTA curve also reveals that the maximum decomposition temperature was at 385.09 °C and 482.10 °C.

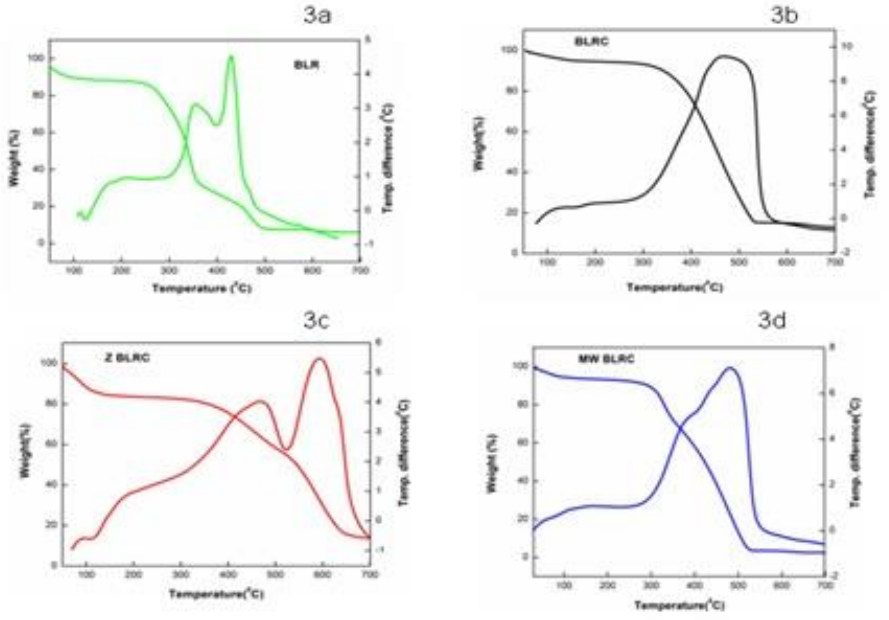

Figure 3: 3a. TGA/DTA plot of BLR, **3b.** TGA/DTA plot of BLRC, **3c.** TGA/DTA plot of Z BLRC & **3d.** TGA/DTA plot of MW BLRC

Table 2: Decomposition temperature with % weight loss obtained from TG curve.

Samples	Temperature of decomposition weight loss (%) of BLR, BLRC, ZBLRC and MWBLRC (°C)						
	100	**200**	**300**	**400**	**500**	**600**	**700**
BLR	10.27	11.91	26.31	73.0	91.97	92.88	93.93
BLRC	2.77	5.33	6.69	23.69	72.45	85.03	86.95
ZBLRC	11.63	16.37	17.5	23.31	41.59	70.14	86.30
MWBLRC	5.51	6.80	10.81	41.96	86.82	96.67	97.47

Table 3. The moisture content and ash content present in the BLR, BLRC, Z BLRC and MW BLRC

Samples	Moisture content (%)	Ash content (%)
BLR	11.91	6.07
BLRC	5.33	13.05
Z BLRC	16.37	13.70
MW BLRC	6.80	2.53

3.3. FE-SEM Analysis

The FE- SEM image of activated charcoal (BLRC, Z BLRC & MW BLRC) before and after dye adsorption was shown in Fig. 4a, 4b, 4c, 4d, 4e & 4f. Well-developed pores have observed on the prepared activated carbons. Chemical ($ZnCl_2$) activated carbon has better porous surface than physical or microwave activated carbon. The SEM image of Z BLRC after adsorption

(Fig. 4e) showed that all the pores are filled by dye molecules.

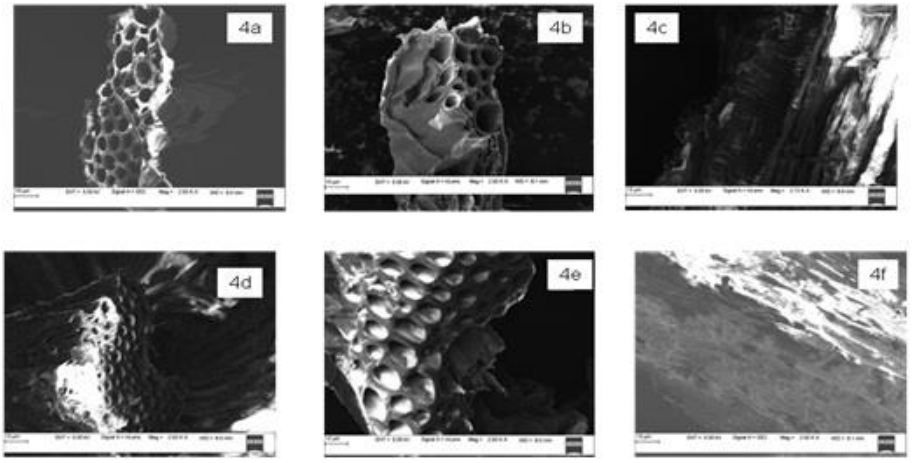

Figure 4: 4a. SEM image of BLRC, **4b.** SEM image Z BLRC, **4c.** SEM image of MW BLRC, **4d.** SEM image of dye adsorbed BLRC, **4e.** SEM image of dye adsorbed Z BLRC, **4f.** SEM image of dye adsorbed MW BLRC

3.4. Adsorption isotherm

Adsorption isotherm relates the amount of dye adsorbed on activated charcoal and the amount of dye remained in the solution at a given temperature and concentration. Adsorption of malachite green on activated charcoal was studied by varying the concentration of malachite green (20 mg/L, 30 mg/L, 40 mg/L, 50 mg/L and 60 mg/L) at constant temperature (30 °C) and agitation time (1h.). Adsorption data were fitted to Freundlich and Langmuir adsorption isotherms.

The logarithmic empirical equation for Freundlich adsorption isotherm is as follows (Prabakaran and Arivoli, 2012).

$$\log(q_e - q_t) = \log q_e - \frac{k_1 t}{2.303} \quad (2)$$

where q_e (mg/g) is the amount of dye adsorbed at equilibrium, k_f and n are the Freundlich constants, C_e (mg/L) is the concentration of dye at equilibrium. The plot of *log* q_e versus *log* C_e is found to be non linear. Hence Freundlich adsorption isotherm is not suited for the system under study. Hence an alternate was made to fit the data to Langmuir adsorption isotherm with the following relation (Sawasdee and Watcharabundit, 2015).

$$\log(q_e - q_t) = \log q_e - \frac{k_1 t}{2.303} \quad (3)$$

where C_e (mg/L) is concentration of dye adsorbed at equilibrium, q_e (mg/g) is the amount of dye adsorbed at equilibrium. q_m or q_{max} value is obtained from the Langmuir adsorption isotherm equation and is calculated as follows:

$$q_{max} = 1/\text{Slope} \quad (4)$$

where q_{max} is the maximum amount of species required for the monolayer adsorption on the activated carbon. *b* is the Langmuir constant. A plot of C_e/q_e versus C_e was drawn and

found to be linear as shown in Fig. 5. From the slope and intercept of above linear plot, value of q_{max} and *b* were evaluated.

The characteristics of Langmuir adsorption isotherm can be expressed in terms of equilibrium parameter R_L ($R_L = (1+bC_0)^{-1}$). Where R_L is the equilibrium parameter, *b* is the Langmuir constant and C_o (mg/L) is the initial dye concentration. Magnitude of R_L value is an indication of favorability of the adsorption process under existing condition. R_L value if lies between 0 and 1 then it is a favorable adsorption and if it equal to unity the plot is linear & R_L if zero the unfavorable adsorption (Sawasdee and Watcharabundit, 2015; Syed, 2011). R_L values are shown in Table 4. and appears to be less than unity favoring the adsorption process.

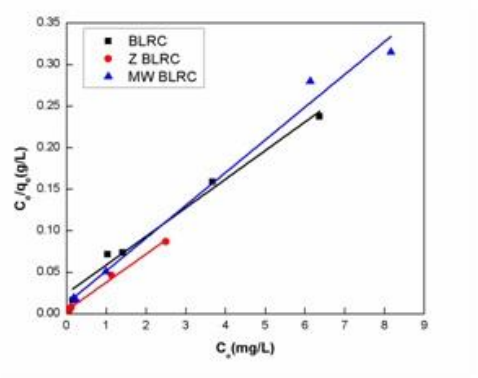

Figure 5. Langmuir adsorption isotherm plot of adsorption of MG on (▪) BLRC, (●) Z BLRC & (▲) MW BLRC

Table 4. Langmuir adsorption isotherm parameters for the adsorption of malachite green on activated carbon (BLRC, Z BLRC & MW BLRC)

Samples	q_{max} (mg/g)	*b*	R_L	R^2
BLRC	29.41	1.41	0.017	0.981
Z BLRC	30.30	11.00	0.002	0.993
MW BLRC	25.64	3.25	0.007	0.984

Regression correlation coefficient value is found to be higher (R^2>0.986) in this case as compared with the value obtained for Freundlich plot. This showed that Langmuir adsorption isotherm model is better fit for the present system than Freundlich adsorption isotherm. The chemical activated banana leaf rim charcoal (Z BLRC) exhibit higher q_{max} value compare to other two types of AC clearly indicating the fact that adsorption capacity of chemical activated charcoal is more compared either to physical or microwave activated charcoal. The amount of species adsorbed or desorbed at equilibrium (q_e) and it was found to between 19 and 20 (mg/g) for all the activated carbon after of 60 min adsorption. The adsorption efficiency of activated charcoal appear in the order Z BLRC > BLRC > MW BLRC. Adsorption capacities of prepared activated carbons were compared with other adsorbent is shown in Table 5.

Table 5. Adsorption capacities of BLRC, Z BLRC & MW BLRC compared with other adsorbent materials

Adsorbent	Adsorption capacity, q_e(mg/g)	Reference
BLRC	19.29	This work
Z BLRC	19.95	This work
MW BLRC	19.50	This work
***Thespesia populnea* bark**	95.49	Prabakaran and Arivoli, 2012
Rice husk	63.85	Rahman *et al.*, 2005
Durian seed	476.19	Ahmad *et al.*, 2014

3.5. Effect of contact time and Kinetics of Adsorption

Adsorption experiment was carried out as a function of time by keeping other parameter as constant. The time range for adsorption is with variation of agitation time 15 min, 30 min, 45 min, 60 min & 75 min. The effect of agitation time on adsorption is shown in Fig. 6.

Fig. 6. illustrates the increase in adsorption process with the increasing agitation time. Here the rate of adsorption found to vary in the order BLRC > Z BLRC > MW BLRC. In case of Z BLRC & MW BLRC the rate increased sharply in the beginning in time of agitation even though amount of adsorption is higher in this case. The MW BLRC exhibited the least capacity among the three activated carbons (Fig. 6).

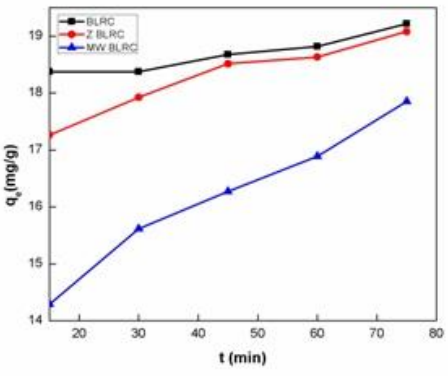

Figure 6: Effect of agitation time on the adsorption of malachite green onto activated carbon [(▪) BLRC, (●) Z BLRC & (▲) MW BLRC]

The two types of kinetic model namely first-order (Reena *et al.*, 2013) and second-order kinetic models (Sun *et al.*, 2013) were used to determine the rate constant for the adsorption of malachite green onto activated carbon (BLRC, Z BLRC & MW BLRC). First-order kinetic equation is as shown below,

$$\log(q_e - q_t) = \log q_e - \frac{k_1 t}{2.303} \quad (5)$$

where q_e (mg/g) is the amount of dye adsorbed at equilibrium and q_t (mg/g) is the amount of dye adsorbed at time t (min); k_1 (1/min) is the first order rate constant. The rate constant is obtained from the slope of the linear plot of $log(q_e - q_t)$ versus t was shown in Fig. 7. And resulted data are shown in Table 6.

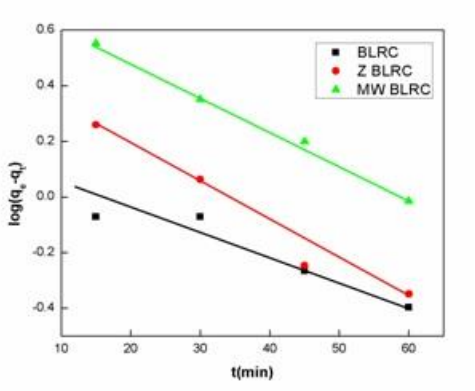

Figure 7. Plots of First- order kinetic model for the adsorption of malachite green onto activated carbon [(▪) BLRC, (●) Z BLRC & (▲) MWBLRC)] at 30 °C.

Table 6. First-order kinetic parameter for the adsorption of malachite green onto activated carbon (BLRC, Z BLRC& MW BLRC)

Samples	R^2	k_1(min^{-1})	q_e (mg/g) (calculated)	q_e (mg/g) (graphical)
BLRC	0.900	0.017	19.41	1.23
Z BLRC	0.968	0.032	19.08	2.91
MW BLRC	0.996	0.731	17.85	5.42

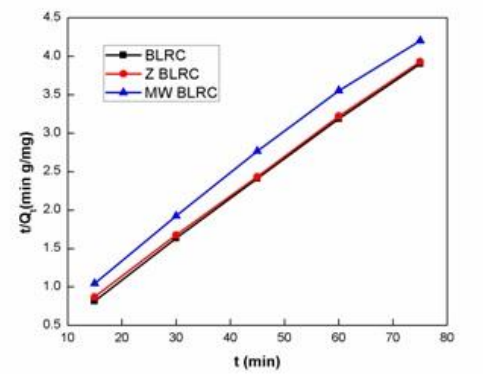

Figure 8. Plots of Second-order kinetics for the adsorption of 40 mg/L of malachite green solution on 0.1g of activated carbon [(▪) BLRC, (●) Z BLRC & (▲) MW BLRC] for 1hr at 30 °C.

From the Table 6, it is clear that experimental value of q_e much smaller than the calculated q_e value informing that the first order rate law not holds good for the present adsorption process.

Second-order kinetics equation (Eq. (6)) was made use to evaluate second order rate constant k_2 for the studied system.

$$\frac{t}{q_t} = \frac{1}{k_2 q_e^2} + \frac{t}{q_e} \quad (6)$$

Second order rate constant k_2 was obtained from the slope of linear plot t/q_t versus t (Fig. 8).

Evaluated Second-order kinetic parameters for dye adsorption are shown in Table 7.

Table 7. Second-order kinetic parameter for the adsorption of malachite green onto activated carbon (BLRC, Z BLRC & MW BLRC)

Samples	R^2	K_2	q_e (mg/g) (calculated)	q_e (mg/g) (graphical)
BLRC	0.999	0.037	19.417	19.221
Z BLRC	0.999	0.022	19.080	19.230
MW BLRC	0.996	0.009	17.853	18.903

The Table 7. Showed a comparable value between the theoretical and experimental q_e values. Nonlinear observed in case of first order plot. The comparable value states that the system belongs to second-order kinetics.

3.8. Effect of temperature on the process of adsorption

The effect of temperature on dye adsorption on three system of AC was studied at temperatures 20 °C, 30 °C, 35 °C & 50 °C. From 20 to 35 °C there was sharp increase in the q_e especially in the case of Z BLRC & MW BLRC. Little effect was observed in the case of BLRC. These are shown in Fig. 9.

Adsorption capacity of activated charcoal (BLRC, Z BLRC & MW BLRC) increases with temperature (Fig. 9.). Thermodynamics of adsorption of dye onto activated carbon was studied and evaluating the thermodynamic parameters such as energy of activation (E_a), change in

enthalpy ($\Delta H^{\ddagger}$), entropy ($\Delta S^{\ddagger}$) and free energy ($\Delta S^{\ddagger}$) were calculated using the following equations (Karaoglu *et al.*, 2010).

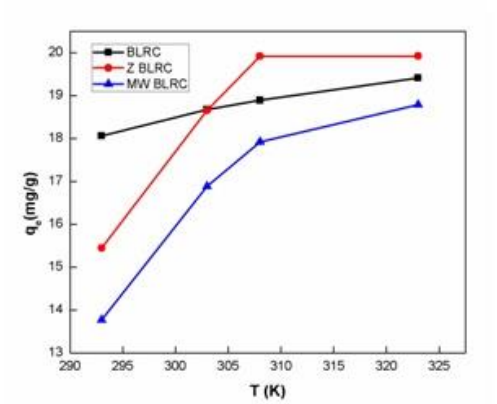

Figure 9. Effect of temperature on dye removal of malachite green by activated charcoal [(▪)BLRC, (●)Z BLRC & (▲) MW BLRC]

$$\log x = \log A - \frac{E_a}{2.303RT} \quad (7)$$

where *x* is concentration of dye after adsorption, E_a is the activation energy, *A* is the Arrhenius parameter, *R* is gas constant and *T* is temperature (*K*). The values of E_a is calculated from the slope of linear plot of *log x* versus *1/T,* (Fig. 10a). Further the thermodynamic parameters like change in enthalpy, entropy and free energy were calculated using absolute theory of rate expression as follows

$$\log\left(\frac{x}{T}\right) = \log\left(\frac{k_B}{h}\right) + \frac{\Delta S^{\ddagger}}{2.303R} - \frac{\Delta H^{\ddagger}}{2.303RT} \quad (8)$$

Where k_B is the Boltzmann constant, h is plank's constant. The change in enthalpy (ΔH‡) and change in entropy (ΔS‡) was calculated from the slope and intercepts of linear plot of log (x/T) versus 1/T as shown in Fig. (10b).

Change in free energy (ΔG‡) can be calculated using the Eq. (9)

$$\Delta G^{\ddagger} = \Delta H^{\ddagger} - T\Delta S^{\ddagger} \quad (9)$$

From the value of (ΔG‡) adsorption constant Kads can be calculated from the equation

$$\Delta G^{\ddagger} = -RT\ln K_{ads} \quad (10)$$

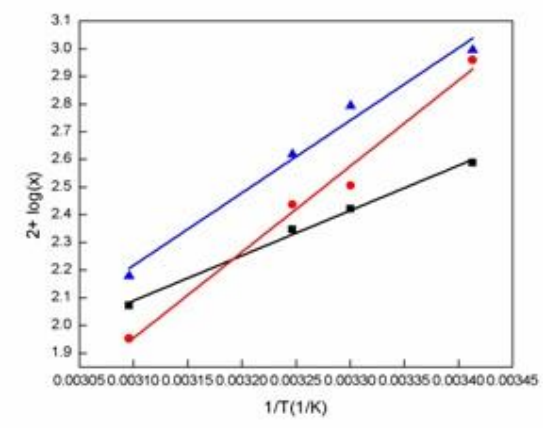

(10a)

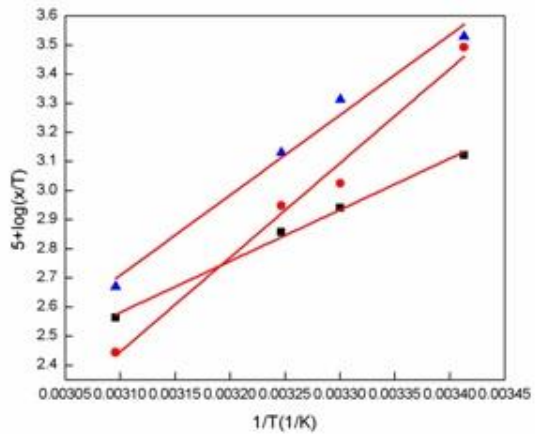

(10b)

Figure 10. Arrhenius plot for the adsorption of malachite green onto (▪)BLRC, (●)Z BLRC & (▲) MW BLRC (**10a)** Plot of 2+log(x) Vs 1/*T*, where x=Concentration of dye after adsorption **(10b)** plot of 5+*log(x/T)* Vs 1/*T*

Table 8. Thermodynamic parameters for the adsorption of malachite green onto [(▪)BLRC, (●) Z BLRC & (▲) MW BLRC]

Samples	E_a (kJ/mol)	$\Delta H^{\ddagger}$ (kJ/mol)	$\Delta S^{\ddagger}$ (kJ/mol/K)	$\Delta G^{\ddagger}$ (kJ/mol)	k_{ads} (kJ/mol)
BLRC	-31.21	-33.77	-0.25	43.77	0.99
Z BLRC	-59.49	-62.06	-0.34	43.15	0.98
MW BLRC	-50.21	-52.78	-0.31	42.01	0.98

From the Table 8. it is clear that the activation energy (E_a) was found to be negative and are comparable for the adsorption process in BLRC, Z BLRC & MW BLRC. The $\Delta H^{\ddagger}$ value for the adsorption process is negative which results that the adsorption of malachite green onto BLRC, Z BLRC & MW BLRC is exothermic. The $\Delta S^{\ddagger}$ value in the present process was found to be negative as required for an adsorption process. On adsorption the degree of randomness or degree of freedom of molecules gets decreased and the particles become stable on the surface

upon adsorption. But the $\Delta G^{\ddagger}$ value which is expected to be negative for a spontaneous process, is not observed in the present case. This could not be explained based on the available data. Value of k_{ads} is almost equal to unity indicating the equilibrium state of the system probably between adsorption and desorption.

4. Conclusions

Activated carbon was successfully synthesized from banana leaf rim using three different activation methods namely physical, chemical and microwave activation. These synthesized carbons were characterized by FT-IR, TGA-DTA and FE-SEM instrument. The FT-IR spectral analysis was carried out to record the functional groups present at the surface of the raw and its activated charcoal. The % weight loss in the sample with temperature was evaluated by the use of TGA & DTA which gave evidence to maximum decomposition composition. Surface morphology of activated carbons gets changed after adsorption of dye adsorption was noticed using FE-SEM. Langmuir adsorption isotherm was better fit for the present adsorption process than Freundlich adsorption isotherm. The present adsorption process followed the second order kinetics. Thermodynamics of adsorption also studied. The study of adsorption of malachite green onto activated carbon could be concluded that adsorption efficiency of chemical activated banana leaf rim charcoal is more compared with physical or microwave activated charcoal.

Acknowledgment

The authors are thankful to the Co-ordinator, DST-FIST Program, USIC and DST-PURSE, Mangalore University for providing instrumental facilities to carry out the present research work. The authors are also thankful to UGC-SAP, Delhi for financial assistance to carry out the present research work.

References

Adamson A.W. (1990), Physical chemistry of surfaces, Fourth Edition, Wiley science, New York.

Ahmad M.A., Ahmad N. and Bello O.S. (2014), Adsorptive removal of malachite green dye using durian seed-based activated carbon, *Water, Air, & Soil Pollution*, **225**(8), 1-18.

Annadurai G., Juang R.S. and Lee D.J. (2002), Use of cellulose wastes for adsorption of dyes from aqueous solutions, *Journal of Hazardous Materials*, **B92**, 263-274.

Bharathi K.S. and Ramesh S.T. (2013), Removal of dyes using agricultural waste as low-cost adsorbents: a review, *Applied water science*, **3**(4), 773-790.

Dewan S. K. (2010), Organic Spectroscopy (NMR, IR, Mass and UV), First Edition, CBS publishers & Distributors Pvt. Ltd, New Delhi.

Dyer J. R. (1987), Applications of Absorption Spectroscopy of Organic Compounds, Sixth Edition, Prentice Hall of India Pvt. Limited, New Delhi.

Idris M.N., Ahmad Z.A. and Ahmad M.A. (2011), Adsorption equilibrium of malachite green dye onto rubber seed coat, *International Journal of Basic and applied Sciences*, **11**(3), 38-42.

Kannan N. and Sundaram M.M. (2001), Kinetics and mechanism of removal of methylene blue by adsorption on various carbons – a comparative study, *Dyes and Pigments*, **51**, 25-40.

Karaoglu M.H., Zor S. and Ugurlu M. (2010), Biosorption of Cr (III) from solutions using vineyard pruning waste, *Chemical Engineering Journal*, **159**(1-3), 98-106.

Mahmoudi K., Hamdi N. and Srasra E. (2014), Preparation and characterization of activated carbon from date pits by chemical activation with zinc chloride for methyl orange adsorption, *Journal of Materials and Environmental Science*, **5**(6), 1758-1769.

Malik P.K. and Saha S.K. (2003), Oxidation of direct dyes with hydrogen peroxide using ferrous ion as catalyst, *Separation and Purification Technology*, **31**(3), 241-250.

Ouajai S. and Shanks R.A. (2005), Composition, structure and thermal degradation of hemp cellulose after chemical treatments, *Polymer Degradation and Stability*, **89**(2), 327-335.

Pavia D. L., Lampman G. M., Kriz G. S. and Vyvyan J. R. (2011), Spectroscopy, Cengage Learning India Private limited, New Delhi.

Prabakaran R. and Arivoli S. (2012), Thermodynamic and isotherm analysis on the removal of malachite green dye using thespesia populnea bark, *Journal of Chemistry*, **9**(4), 2575-2588.

Rahman I.A., Saad B., Shaid S. and Rizal E.S.S. (2005), Adsorption characteristics of malachite green on activated carbon derived from rice husks produced by chemical-thermal process, *Bioresource Technology*, **96**(14), 1578-1583.

Reena K., Goyal M., Bhagat M., Chaudhary G.R. and Sharma M.L. (2013), Influence of carbon-oxygen surface groups on adsorptive removal of malachite green dye from water, *Indian Journal of Chemical Technology*, **20**(2), 87-94.

Sawasdee S. and Watcharabundit P. (2015), Equilibrium, Kinetics and Thermodynamic of Dye Adsorption by Low - cost Adsorbents, *International Journal of Chemical Engineering and Applications*, **6**(6), 444-449.

Sun D., Zhang Z., Wang M. and Wu Y. (2013), Adsorption of Reactive Dyes on Activated Carbon Developed from *Enteromorpha prolifera*, *American Journal of Analytical Chemistry*, **4**(7A), 17-26.

Syed S.P.S. (2011), Study of the Removal of Malachite Green from Aqueous Solution by using Solid Agricultural Waste, *Research Journal of Chemical Sciences*, **1**(1), 88-104.

Zhang H., Wang Y., Bai P., Guo X. and Ni X. (2016), Adsorptive Separation of Acetic Acid from Dilute Aqueous Solutions: Adsorption Kinetic, Isotherms, and Thermodynamic Studies, *Journal of chemical & engineering data*, **61**(1), 213-219.